DOI: 10.1002/ejic.200501148

A Theoretical Study on Structures, Bonding Energies and Aromaticity of Two New Series of Dinuclear Phosphametallocenes: (η^5-P_5)MM′(η^5-P_5) and (η^5-C_5H_5)MM′(η^5-P_5) (M, M′ = Zn, Cd)

Zi-Zhong Liu,[a,b,c] Wei Quan Tian,*[a] Ji-Kang Feng,*[a,c] Gang Zhang,[a] Wei-Qi Li,[a] Yan-Hong Cui,[a] and Chia-Chung Sun[a]

Keywords: Dinuclear phosphametallocenes / Structures / Bonding energies / Aromaticity / Density functional theory

The equilibrium geometries, the energies, the harmonic vibrational frequencies, and the nucleus independent chemical shifts (NICSs) of the ground state of (η^5-P_5)MM′(η^5-P_5) and (η^5-C_5H_5)MM′(η^5-P_5) (M, M′ = Zn, Cd) are calculated by the hybrid density functional method B3LYP with LANL2DZ basis sets. The analysis of energy and harmonic frequencies on the equilibrium geometries of both series dinuclear deca- and pentaphosphametallocenes shows that all the minima with singlet electronic state have an staggered ($9° \leq D_{(E-M-M-E')} \leq 36°$) conformation except for the eclipsed $CpCd_2(P_5)$ (C_{5v}), and all the D_{5h} and the D_{5d} symmetric conformations are transition states while the energy differences between the most stable minimum and the transition states are very small ($\leq$ 0.1 kcal/mol), thus, the rotation of the P_5 ring about M–M bond in all complexes is almost free. The analysis of the NBO, the Laplacian of the electron density, the electrostatic interaction energy, the bonding energy decomposition, and the molecular orbital correlation diagrams for the two series complexes reveals that the properties of all the dinuclear phosphametallocenes investigated are similar to that of the dizinc metallocenes. The M–M (or M–M′) bond in the dinuclear phosphametallocenes is a weak σ covalent bond, and the magnitude of bonding energy of the M–M (or M–M′) bond correlates with the energy difference between the energy of HOMO in M(η^5-P_5) (or MCp) (^2A, C_{5v}) fragment and the energy of HOMO-2 in [MM′(η^5-P_5)$_2$] (^1A, D_5, or D_{5h}) [or (η^5-P_5)MM′Cp (^1A, C_5, or C_{5v})] (M, M′ = Zn, Cd). The strength of the M–M (or M–M′) bond plays a decisive role on the stability of the dinuclear phosphametallocenes. However, the M–(η^5-P_5) (or M–Cp) bonding mainly is ionic. Among the different dinuclear phosphametallocenes with the same ligands, the bonding energies of the M–M (or M–M′) bond and of the M–(η^5-P_5) (or M–Cp) bond decrease as M varying from Zn to Cd. Among the different phosphametallocenes with the same metals, the bonding energies of the M–M (or M–M′) bond and the M–ligand bond increase with ligand varying from the (η^5-P_5) to the Cp. The negative NICSs indicate that all dinuclear phosphametallocenes have aromaticity. The various dissected bond NICS contributions reveal that the NICS contributions of the metal–ligand bond, the metal–metal bond, and the metal lone pair electrons to the overall aromaticity in the Zn-containing dinuclear phosphametallocenes are different from their counterpart contributions in the Cd-containing dinuclear phosphametallocenes, such difference causes that the overall NICSs of the Zn-containing dinuclear phosphametallocenes are more negative than that of the Cd-containing dinuclear phosphametallocenes.

(© Wiley-VCH Verlag GmbH & Co. KGaA, 69451 Weinheim, Germany, 2006)

1. Introduction

The successful synthesis of the linear organometallic molecule, decamethyldizincocene, [Zn_2(η^5-Cp*)$_2$] (Cp* = C_5Me_5) by Resa and co-workers recently,[1,2] has provided inorganic chemists with their first example of a stable organometallic compound with a homonuclear metal Zn–Zn bond, and has been considered as a new frontier of the dinuclear metallocenes study.[3] One motivation of the present study is stimulated by the new synthesis routes[4,5] and theoretical studies on the structures, the bond interactions,[2] and the vibrational signatures of the Zn–Zn stretching mode in the novel molecule.[6] The analogous dinuclear metallocenes, such as $CpCu_2Cp$ and $CpNi_2Cp$,[7] [M_2(η^5-Cp^X)$_2$] (M = Zn and Cd, Cp^X = C_5Me_5 and C_5H_5),[8] and the dinuclear cyclopentadienylcobalt carbonyls[9] were investigated. The homodinuclear metallocenes, [M_2-(η^5-Cp)$_2$] (M = Be, Mg, and Ca),[10] and the heterodinuclear metallocenes, CpE–MCp (E = B, Al, Ga; M = Li, Na, K),[11] and Cp–Zn–Cd–Cp[12] were studied as well. These studies are fascinating and encourage our further explorations of analogous homodinuclear and heterodinuclear phosphametallocenes.

Since the first synthesis of pentamethylpentaphosphaferrocene by Scherer et al.[13] and pentaphosphacyclopentadi-

[a] State Key Laboratory of Theoretical and Computational Chemistry, Institute of Theoretical Chemistry, Jilin University, Changchun 130023, China
[b] Chemistry and Environment Science College of Inner Mongolia Normal University, Huhhot, 010022 China
[c] The College of Chemistry, Jilin University, Changchun 130023, China

 © 2006 Wiley-VCH Verlag GmbH & Co. KGaA, Weinheim

enide anion (P_5^-) by Baudler and co-workers,[14,15] the structure of pentaphosphametallocene and the aromaticity of polyphosphaphospholes and P_5^- have attracted much attention from the chemistry community by the fact that metallocene and analogous organometallic compounds have been found in many applications, e.g. synthetic reagents, catalysts of polymerization and hydrogenation of olefin, and building blocks for new materials.[16–32] Experimental and computational studies suggested that the pentaphospholyl anion, P_5^-, is aromatic, as cyclopentadienyl anion, Cp^-.[16–21,33,35] Recent synthesis and X-ray structural analysis of the homoleptic sandwich complex with pentaphospholyl anion ligands, $[Ti(\eta^5\text{-}P_5)_2]^{2-}$,[34] gave a new impetus to the versatile chemistry of phosphametallocenes. The structure, bonding and aromaticity of the decaphosphametallocenes $[Ti(\eta^5\text{-}P_5)_2]^{2-}$ were theoretically reported by Lein et al.[35] and our group,[33] respectively. $[Ti(\eta^5\text{-}P_5)_2]^{2-}$ is aromatic with stronger aromaticity.[33] However, it has not been investigated, to the best of our knowledge, on the stabilities, electronic structures and aromaticity of the homodinuclear phosphametallocenes: $[M_2(\eta^5\text{-}P_5)_2]$ and $(\eta^5\text{-}C_5H_5)\text{-}M_2(\eta^5\text{-}P_5)$, (M = Zn, Cd), and the heterodinuclear phosphametallocenes: $(\eta^5\text{-}P_5)MM'(\eta^5\text{-}P_5)$ and $(\eta^5\text{-}C_5H_5)\text{-}MM'(\eta^5\text{-}P_5)$ (M, M′ = Zn, Cd).

To better understand the bonding nature of the M–M (or M–M′) and of the M–$(\eta^5\text{-}P_5)$ in titled molecules, it is necessary to investigate the geometric and electronic structures and binding energies of a series of complexes. The purpose of this paper is to exhibit the features of structures, the bonding energies and the aromaticity of the homodinuclear and the heterodinuclear phosphametallocenes within density functional theory (DFT). Meanwhile, the qualitative analysis of the molecular orbital correlation diagram and the Laplacian of the electron density $[\nabla^2\rho(r)]$ of the atom in molecule (AIM)[36–38] are performed to characterize the bonding features of the interaction and to provide insights into the influences of metals and ligands on the bonding character and aromaticity in both series of complexes.

2. Computational Methods

The DFT geometry optimizations at B3LYP/gen [P: 6-311+G(2d), C, H: 6-311+G(d,p), Zn, Cd: LANL2DZ] level of theory are carried out on several symmetrical conformations [eclipsed (D_{5h} or C_{5v}), staggered (D_{5d}, D_5 and C_5)] of the homodinuclear with homo-ligands, the heterodinuclear with homo-ligands, the homodinuclear with hetero-ligands and the heterodinuclear with hetero-ligands sandwich-like complexes with pentaphospholyl ligands and Cp ligand: $(\eta^5\text{-}P_5)M_2(\eta^5\text{-}P_5)$, $(\eta^5\text{-}P_5)MM'(\eta^5\text{-}P_5)$, $(\eta^5\text{-}C_5H_5)\text{-}M_2(\eta^5\text{-}P_5)$ and $(\eta^5\text{-}C_5H_5)MM'(\eta^5\text{-}P_5)$ (M, M′ = Zn, Cd), respectively (as shown in Figure 1). In order to check our computational reliability and to compare the differences between $[M_2(\eta^5\text{-}P_5)_2]$ and $[M_2(\eta^5\text{-}Cp)_2]$ (M = Zn, Cd), we optimized the dinuclear metallocene $[M_2(\eta^5\text{-}Cp)_2]$ (D_{5h}, D_{5d}, D_5) reported by Xie et al.[8] The vibrational frequencies were calculated and the DFT wavefunction instabilities were checked at the same level of theory. The nature of all the stationary points on the potential energy surface (PES) are verified with the vibrational frequency calculations in which Hessian (the second order derivatives of total energy with respect to nuclear coordinates on PES) are calculated. If all eigenvalues in Hessian are positive for a stationary point, this stationary point is a minimum on the PES. One or more negative eigenvalues of a stationary point indicates a saddle point on PES. The natural bond orbital (NBO)[39] analyses are performed to gain insight into the bonding pattern of these complexes. The bond lengths, the natural atomic charges, the vibrational frequencies, the Wiberg bond index (WBI) in Natural Atomic Orbital (NAO), and the Laplacian of the electron density $\nabla^2\rho(r)$ of the constituent atoms of the complexes under investigation are calculated. The nucleus-independent chemical shift (NICS), as an index of aromaticity, at different positions in every structure are predicted with GIAO-B3LYP//B3LYP/gen [P: 6-311+G(2d), C, H: 6-311+G(d,p), Zn,Cd: LANL2DZ]. The NICS(0) is computed at the ring center, the NICS(1) is computed at 1 Å above the ring center, and the NICS(–1) is computed at 1 Å beneath the ring center. All of the NICS dissections of various bonds and cores are computed by NBO3.1.[39,40] All the calculations were carried out with the Gaussian03 program package.[39] The molecular orbitals (MOs) of the complexes are plotted with MOLDEN 4.0.[40]

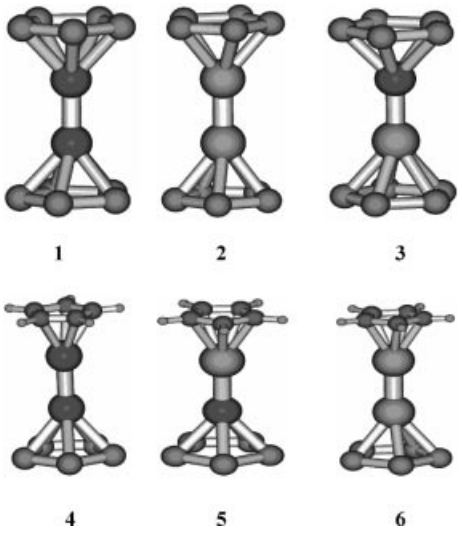

Figure 1. Molecular structures. 1 $(\eta^5\text{-}P_5)Zn_2(\eta^5\text{-}P_5)$, 2 $(\eta^5\text{-}P_5)\text{-}Cd_2(\eta^5\text{-}P_5)$, 3 $(\eta^5\text{-}P_5)ZnCd(\eta^5\text{-}P_5)$, 4 $CpZn_2(\eta^5\text{-}P_5)$, 5 $CpCd_2(\eta^5\text{-}P_5)$, 6 $CpCdZn(\eta^5\text{-}P_5)$.

3. Results and Discussions

3.1 Geometric Structures

Table 1 and Table 2 list the bond lengths, the WBI in NAO, the natural atomic charge (NAC) $q|e|$, the staggered angle ($D_{(E\text{–}M\text{–}M\text{–}E')}$) between the two P_5 (or Cp) rings, and the Laplacian of the electron density $\nabla^2\rho(r)$ between the M

 © 2006 Wiley-VCH Verlag GmbH & Co. KGaA, Weinheim

atoms and between the M atom and the ligand ring for the homodinuclear phosphametallocenes, $[M_2(\eta^5\text{-}P_5)_2]$ and $(\eta^5\text{-}C_5H_5)M_2(\eta^5\text{-}P_5)$ (M = Zn and Cd) and the heterodinuclear phosphametallocenes, $(\eta^5\text{-}P_5)MM'(\eta^5\text{-}P_5)$ and $(\eta^5\text{-}C_5H_5)MM'(\eta^5\text{-}P_5)$ (M, M′ = Zn, Cd).

All the minima of the dinuclear phosphametallocenes with singlet electronic state, including the homodinuclear phosphametallocenes, $[M_2(\eta^5\text{-}P_5)_2]$ and $(\eta^5\text{-}C_5H_5)M_2(\eta^5\text{-}P_5)$ (M = Zn and Cd) and the heterodinuclear phosphametallocenes, $(\eta^5\text{-}P_5)MM'(\eta^5\text{-}P_5)$ and $(\eta^5\text{-}C_5H_5)MM'(\eta^5\text{-}P_5)$ (M, M′ = Zn, Cd), have an staggered ($9° \leq D_{(E\text{–}M\text{–}M\text{–}E')} \leq 36°$) conformation except for the eclipsed $CpCd_2(P_5)$ (C_{5v}, $D_{(E\text{–}M\text{–}M\text{–}E')} = 0°$). All the D_{5h} and D_{5d} symmetric conformations are transition states while the energy differences between the minima and the transition states are very small (≤ 0.1 kcal/mol). This is in agreement with the energy differences (0.01 kcal/mol) between the minima in D_{5d} symmetry and the transition states in D_{5h} symmetry in CpZnZnCp,[8] CpNiNiCp,[8] and $[M_2(\eta^5\text{-}Cp)_2]$ (M = Be, Mg, Ca).[10] These results indicate that the rotation of P_5 ring about the M–M bond in all complexes is almost free. It suggests that the $[M_2(\eta^5\text{-}P_5)_2]$ (M = Zn, Cd) may be similar to CpMMCp (M = Zn, Cd).

As shown in the Table 1, the Zn–Zn bond lengths in our predictions, 2.487, 2.476, and 2.466 Å in $[Zn_2(\eta^5\text{-}P_5)_2]$, $[CpZn_2(\eta^5\text{-}P_5)]$, and $CpZn_2Cp$, respectively, are close to

Table 1. Bond lengths, natural atomic charge, WBI in NAO, staggered angle, electrostatic interaction energies ($V_{Ep\text{–}M_2^{2+}(M)}$) and the Laplacian of the electron density $\nabla^2\rho(r)$ between M atoms and between M atom and ligand ring for the local minima of $(\eta^5\text{-}P_5)M_2(\eta^5\text{-}P_5)$, $CpM_2(\eta^5\text{-}P_5)$ and CpM_2Cp (M = Zn and Cd) predicted at B3LYP/Gen [P: 6-311+G(2d), C, H: 6-311+G(d,p), Zn,Cd: LANL2DZ] level.

	$[M_2(P_5)_2]$			$CpM_2(P_5)$				CpM_2Cp		
	P_5^-	$Zn(P_5)$	$Cd(P_5)$	$Zn(P_5)$	ZnCp	$Cd(P_5)$	CdCp	Cp	ZnCp	CdCp
$r_{E\text{–}E}$[a]	2.119	2.137	2.139	2.135	1.423	2.137	1.424	1.415	1.422	1.423
$r_{Ep\text{–}M}$		2.126	2.370	2.157	2.050	2.392	2.162		2.067	2.309
$r_{M\text{–}M}$		2.487	2.764	2.476		2.747			2.466	2.729
q_{Ep}	–1.00	–0.79	–0.80	–0.80	–0.87	–0.81	–0.85	–1.00	–0.87	–0.86
$q_{M_2^{2+}}$		1.58	1.59	1.67		1.70			1.74	1.72
$WBI_{E\text{–}E}$	1.406	1.360	1.361	1.365	1.383	1.368	1.382	1.405	1.385	1.384
$WBI_{M\text{–}M}$		0.765	0.765	0.809		0.801			0.864	0.852
$WBI_{M\text{–}E}$		0.063	0.050	0.058	0.048	0.052	0.052		0.048	0.048
$D_{(E\text{–}M\text{–}M\text{–}E')}$ [°]		18.0	22.1	27.0		0.0			18.0	0
Group	D_{5h}	D_5	D_5	C_5		C_{5v}		D_{5h}	D_5	D_{5h}
$\nabla^2\rho(r_{E\rho}\text{–}M)$		0.054	0.061	0.046	0.139	0.059	0.130		0.114	0.126
$\nabla^2\rho(r_{M\text{–}M})$		0.020	0.061	0.031		0.066			0.021	0.072
$V_{E\rho\text{–}M}$[b]		0.29	0.27	0.26	0.41	0.25	0.37		0.37	0.32

[a] E = P or CH, Ep = η^5-P_5 or Cp. [b] $V_{Ep\text{–}M^+}$ is the electrostatic interaction energies between Ep and M, $V_{Ep\text{–}M_2^{2+}} = k\frac{q_{M_2^{2+}}q_{Ep}}{r_{M_2^{2+}\text{–}Ep}}$, or $V_{Ep\text{–}M^{2+}} = k\frac{q_{M^{2+}}q_{Ep}}{r_{M^{2+}\text{–}Ep}}$, the k unit is $-\frac{1}{4\pi\varepsilon_0}$. The $r_{M_2^{2+}\text{–}Ep}$ (or $r_{M^{2+}\text{–}Ep}$) is distance between the center of Ep ring and M_2^{2+}(or M^{2+}).

Table 2. Bond lengths, natural atomic charge, WBI in NAO, staggered angle, electrostatic interaction energies ($V_{Ep\text{–}M_2^{2+}(M)}$) and the Laplacian of the electron density $\nabla^2\rho(r)$ between M atoms and between M atom and ligand ring for the local minima of $(\eta^5\text{-}P_5)ZnCd(\eta^5\text{-}P_5)$, $CpCdZn(\eta^5\text{-}P_5)$ and CpZnCdCp predicted at B3LYP/Gen level.

	$(P_5)ZnCd(P_5)$		$CpCdZn(P_5)$		CpZnCdCp	
	$(P_5)Zn$	$Cd(P_5)$	$Zn(P_5)$	CdCp	CpZn	CdCp
$r_{E\text{–}E}$[a]	2.138	2.138	2.137	1.424	1.423	1.423
$r_{Ep\text{–}M}$	2.127	2.377	2.154	2.295	2.027	2.275
$r_{M\text{–}M}$	2.625		2.612		2.597	
q_{Ep}	– 0.79	– 0.80	–0.80	–0.85	–0.87	–0.86
$q_{M_2^{2+}}$	0.74	0.85	0.68	0.97	0.85	0.88
$WBI_{E\text{–}E}$	1.360	1.365	1.364	1.382	1.384	1.384
$WBI_{M\text{–}M'}$	0.760		0.793		0.856	
$WBI_{M\text{–}E}$	0.059	0.060	0.028	0.050	0.047	0.047
$D_{(E\text{–}M\text{–}M'\text{–}E')}$	9.0		36.0		36.0	
Group	C_5		C_{5v}		C_5	
$\nabla^2\rho(r_{Ep\text{–}M})$	0.053	0.061	0.053	0.130	0.114	0.127
$\nabla^2\rho(r_{M\text{–}M})$	0.040		0.043		0.045	
$V_{Ep\text{–}M^+}$[b]	0.28	0.29	0.25	0.36	0.37	0.33

[a] E = P or CH, Ep = η^5-P_5 or Cp. [b] $V_{Ep\text{–}M^+}$ is the electrostatic interaction energies between Ep and M^+ in MM'^{2+}, $V_{Ep\text{–}M^{2+}} = k\frac{q_{M^{2+}}q_{Ep}}{r_{M^+\text{–}Ep}}$, the k unit is $-\frac{1}{4\pi\varepsilon_0}$. The $r_{M^+\text{–}Ep}$ is distance between the center of Ep ring and M^+(or M^{2+}) in MM'^{2+}(M, M′ = Zn, Cd).

 © 2006 Wiley-VCH Verlag GmbH & Co. KGaA, Weinheim

each other, and decrease with the ligand varying from P_5 to Cp. The change of the Cd–Cd bond length in $[Cd_2(\eta^5\text{-}P_5)_2]$, $CpCd_2(\eta^5\text{-}P_5)$, and $CpCd_2Cp$ is analogous to that of the Zn–Zn bond length in three Zn-containing complexes, while the Cd–Cd bond length is longer than Zn–Zn in their counterparts. The Zn–(η^5-P_5) (2.126 Å) distance in $[Zn_2(\eta^5\text{-}P_5)_2]$ is longer than the Zn–Cp (2.067 Å) distance in $CpZn_2Cp$, and the Cd ligand distance is analogous to the Zn ligand distance. The M–(η^5-P_5) distance in $[M_2(\eta^5\text{-}P_5)_2]$ is shorter than the M–Cp distance in $[CpM_2(\eta^5\text{-}P_5)]$ (M = Zn and Cd). However, the Zn ligand distance is shorter than the Cd ligand distance. This indicates that the interaction between the M atom and the η^5-P_5 rings is similar to that between the M atom and the Cp rings, while the interaction in the former is slightly smaller than that in the latter, and the interaction between the Zn atoms and the ligand rings is stronger than that between the Cd atoms and the ligand rings. The interaction trends between the M atom and the ligand rings is completely in the same trends as the electrostatic interaction energies between Ep and M^+ as V_{Ep-M^+} listed in Table 1, in which the electrostatic interaction between the M atom and the η^5-P_5 rings is similar to that between the M atom and the Cp rings, but the electrostatic interaction in the former is slightly smaller than that in the latter, and the electrostatic interaction between the Zn atoms and the ligand rings is stronger than that between the Cd atom and the ligand rings. The analyses of the WBI and the $\nabla^2\rho(r)$[36–39,42] between M atoms, and between M atoms and the ligand rings, indicate that the M–M bond is predominantly weakly covalent, and the M–(η^5-P_5) bonding is mainly of ionic, and the bond strengths of the M–M bond in the two series complexes are very close.

As shown in Table 2, in the heterodinuclear phosphametallocenes, the magnitudes of bond length, the WBI and the$\nabla^2\rho(r)$ between Zn and Cd, and between M and Ligands, reveal that the Zn–Cd bond is a weak covalent, and the M–Ligand bond is main ionic, too. The electrostatic interaction between the M atom and the η^5-P_5 rings is slightly weaker than the interaction between the M atom and Cp ring, while the covalent interaction in the former is stronger than that in the latter.

Comparing the r_{P-P} in the homodinuclear or the heterodinuclear phosphametallocenes with that in the η^5-P_5^-(D_{5h}) ion, in which all P–P bonds are equal, we can find that the r_{P-P} in the former is longer than that in the latter. According to the fact that the bond lengths of r_{P-P} lie between the single P–P (≥ 2.21 Å) and the double P=P (≤ 2.02 Å) bonds,[21,34] and the calculated adjacent P–P WBI in all molecules from the NBO analyses is in the range of 1.3–1.4, which is between the standard values of single-bond (1.0) and double-bond (2.0), we can infer that the building block P_5 in all $[M_2(\eta^5\text{-}P_5)_2]$ complexes has conjugated P–P bonds, and all molecules have aromaticity according to the P–P bond lengths.

3.2 Dissociation Energies

On the basis of the NBO charge and the sign of the $\nabla^2\rho(r)$ in the complexes, in which the M_2 unit (or M) and the (η^5-P_5) building block have nearly +2 |e| (or +1 |e|) and –1 |e| charges, respectively, and the $\nabla^2\rho(r) > 0$, the interaction between M and the (η^5-P_5) is mainly ionic. In order to compare their stabilities, eight dissociation pathways are proposed, and their dissociation energies are calculated for each pathway as shown in Table 3 and Table 4.

The pathways (1) and (4) involve breaking of the M–M and the M–M′ (M,M′ = Zn, Cd) bond. From Table 3 and Table 4, according to the magnitude of the dissociation energies of the M–M (M = Zn, Cd) bond, except for that of the Cd–Cd bond in $[Cd_2(\eta^5\text{-}P_5)_2]$, the dissociation energies of the M–M (or M–M′) (M = Zn, Cd) bond in the complexes and in the CpM_2Cp (D_5 or D_{5h}) are very close, especially, that of the Zn–Zn bond. These results indicate that the stability of three complexes is analogous to $CpZn_2Cp$ which was successfully synthesized by Resa et al.,[1] that

Table 3. Dissociation energies for (η^5-P_5)M_2(η^5-P_5), CpM_2(η^5-P_5) and CpM_2Cp (M = Zn, Cd) at 3LYP/Gen level of theory.[a]

Dissociation pathway	$[(Ep)_2M_2]$		$C_pM_2(P_5)$		$C_pM_2C_p$	
	Zn	Cd	Zn	Cd	Zn	Cd
(1) $[(Ep)_2M_2] \xrightarrow{\Delta E_1} Ep\,M + MEp$	51.4	44.6	53.8	47.1	55.4	49.1
(2) $[(Ep)_2M_2] \xrightarrow{\Delta E_{21}} EpM_2^{\prime} + Ep^-$	121.3	104.9	154.9[b] (124.9)[c]	143.8[b] (115.0)[c]	164.8	142.5
$EpM_2^+ \xrightarrow{\Delta E_{22}} M_2^{2+} + Ep^-$	278.8	251.9	315.6[b] (278.8)[c]	251.9[b] (280.9)[c]	315.6	280.9
(3) $[(Ep)_2M_2] \xrightarrow{\Delta E_3} M_2^{2+} + 2\,Ep^-$	400.1	367.7	440.6	395.7	480.5	423.2

[a] All EpM_2^+ have C_{5v} symmetry and $^2A_1$ electronic state, all EpM have C_{5v} symmetry and $^2A_1$, electronic state, all Ep and Cp have D_{5h} symmetry and $^1A_{1g}$ electronic state; M_2^{2+} have $^1S_{gg}$ electronic state. [b] The dissection energy of P_5M_2–Cp as the equation $CpM_2P_5 \rightarrow P_5M_2^+ + Cp^-$. [c] The dissection energy of CpM_2–P_5 as the equation $CpM_2P_5 \rightarrow CpM_2^+ + P_5^-$.

 © 2006 Wiley-VCH Verlag GmbH & Co. KGaA, Weinheim

Table 4. Dissection energies for (η^5-P_5)ZnCd(η^5-P_5), CpZnCd(η^5-P_5) and CpZnCdCp at B3LYP/6-311+G(d,p) level of theory.[a]

Dissociation pathway	$(P_5)ZnCd(P_5)$		$C_pCdZn(P_5)$		C_pZnCdC_p	
	Zn—P_5 Cd—P_5	Cd—P_5 Zn—P_5	Cd—C_p Zn—C_p	Cd—C_p Zn—C_p	Zn—P_5 Cd—C_p	Cd—C_p Zn—P_5
(4) $[(Ep)_2ZnCd] \xrightarrow{\Delta E_4}$ Ep Zn + CdEp	47.8		50.15		64.3	
(5) $[(Ep)_2ZnCd] \xrightarrow{\Delta E_{51}} EpZnCd^+ + Ep^-$	122.6	114.1	203.3	203.3	115.3	142.02
$EpZnCd^+ \xrightarrow{\Delta E_{52}} ZnCd^{2-} + Ep^-$	260.4	268.8	302.6	302.6	302.6	268.84
(6) $[(Ep)_2ZnCd] \xrightarrow{\Delta E_6} ZnCd^{2+} + 2\ Ep^-$	329.0		410.9		469.9	

[a] All $EpZnCd^+$ have C_{5v} symmetry and ^2A electronic state, all EpM (M = Zn and Cd) have C_{5v} symmetry and $^2A_1$ electronic state; all Ep and Cp have D_{5h} symmetry and $^1A_{1g}$ electronic state; $ZnCd^{2+}$ has ^1S_g electronic state.

they can be synthesized. However, the dissociation energy of the M–M (M = Zn, Cd) bond in the homodinuclear phosphametallocenes or of the M–M′ (M, M′ = Zn, Cd) bond in heterodinuclear phosphametallocenes increases with the number of Cp ligands, i.e. $[M_2(P_5)_2] < CpM_2(P_5) < CpM_2Cp$, and $(P_5)ZnCd(P_5) < CpCdZn(P_5) < CpZnCdCp$, though their energy differences are very small, only about 1.6–2.5kcal/mol in homodinuclear phosphametallocenes, and bout 1.6–14.1 kcal/mol in heterodinuclear phosphametallocenes. Comparison the dissociation energy of the dinuclear phosphametallocenes with that of the counterpart metallocenes indicates that the M–M (M = Zn, Cd) bond and the M–M′ (M, M′ = Zn, Cd) bond in phosphametallocenes are slightly weaker than that in the counterpart metallocenes. Comparison of the dissociation energy of the Zn–Zn bond in the dizinc phosphametallocenes with that of the Cd–Cd bond in the dicadmium phosphametallocenes reveals that the Zn–Zn bond is stronger than the Cd–Cd bond. Thus the dizinc phosphametallocenes are more stable than the dicadmium phosphametallocenes. These results are consistent with the WBI_{M-M} analysis that the M–M (M = Zn, Cd) bond in phosphametallocenes is less stable than that in metallocenes which is a weak covalent bond.

Pathway (2) or (5) in Table 3 and Table 4 involves the breaking of the metal–ligand bonds in two-step dissection, while pathway (3) or (6) involves the breaking of the two metal–ligand bonds in one-step dissection. As shown in Table 3 and Table 4, the first and the second dissociation energies of the metal–ligand bonds in pathway (2) [or pathway (5)] are not equal. The first dissociation energy (E_{21}) is much smaller than the second one (E_{22}). This indicates that the first group metal–ligand bonds are easier to break while the second group metal–ligand bonds are more stable after the first step dissection. ΔE_{21}, ΔE_{22}, and 1/2 ΔE_3 in Table 3 (or ΔE_{51}, ΔE_{52} and 1/2 ΔE_6 in Table 4) giving the first, the second and the average dissociation energy of the M_2^{2+} ($^1S_{gg}$) with P_5^- ($^1A_1$, D_{5h}) in the dinuclear phosphametallocenes are very large, thus indicating that the bonding of M_2^{2+} with P_5^- is very strong in those systems.

Comparing the first, the second and the average dissociation energy of the metal–P_5 bonds in the dinuclear phosphametallocenes with those of the metal–Cp bonds in the dinuclear metallocenes, it can be inferred that the interaction between M_2^{2+} and P_5^- is close to (and slightly weaker than) that between M_2^{2+} and Cp^-. Furthermore, this interaction is consistent with the electrostatic interaction, in which the V_{Ep-M^+} between the M cation and the P_5 anion in the dinuclear phosphametallocenes is close to that between the M cation and the Cp anion in the dinuclear metallocenes, though the magnitude in the former is slightly smaller. However, this is opposite to the conclusion of the WBI analysis between the metal and the ligand (P_5 or Cp), in which the WBI between the M cation and the P_5 anion in the dinuclear phosphametallocenes is larger than that between the M cation and the Cp anion in the dinuclear metallocenes. It further illustrates that the electrostatic interaction between the metal and the ligand (P_5 or Cp) in the dinuclear phosphametallocenes dominates the overall interactions.

Comparison of the dissociation energy of the Zn–P_5 bonds in $[Zn_2(\eta^5\text{-}P_5)_2]$ (D_5) with that of the Cd–P_5 bonds in $[Cd_2(\eta^5\text{-}P_5)_2]$ (D_5), and comparison of the dissociation energy of the Zn–P_5 bonds with that of Cd–P_5 bonds in $[ZnCd(\eta^5\text{-}P_5)_2]$ (C_5) show that the dissociation energy of the Zn–P_5 bonds is larger than that of the Cd–P_5 bonds. The analysis of electrostatic interactions (the V_{Ep-M^+} listed in Table 3 and Table 4) also supports this observation.

Comparison of the dissociation energy of the M–M (or M–M′; M, M′ = Zn, Cd) bond with that of the M–(η^5-P_5) bonds in the dinuclear phosphametallocenes, in which the magnitude of the former from 45 to 64 kcal/mol is much smaller than that of the latter from 105 to 316 kcal/mol, reveals that the strength of the M–M bond is much weaker than that of the M–(η^5-P_5) bond. Therefore, the stability of the dinuclear phosphametallocenes mainly depend on the

 © 2006 Wiley-VCH Verlag GmbH & Co. KGaA, Weinheim

magnitude of the M–M bond strength, i.e. the strength of the M–M bonding plays a more dominant role to the stability of the dinuclear phosphametallocenes.

3.3 Electronic Structures

Analyses of the WBI, the $\nabla^2\rho(r)$ and the dissociation energy of the M–M (or M–M′) and the M–(η^5-P_5) in the dinuclear phosphametallocenes reveal that the M–M (or M–M′) bond is covalent and the interaction between M and ligands is mainly ionic. In order to gain insight into the covalent nature of the M–M (or M–M′) bond and to explore the reason for the stabilities of the dinuclear phosphametallocenes, a correlation diagram between the M(η^5-P_5) fragments is depicted in Figure 2, in which several most relevant MOs in M(η^5-P_5) and [M_2(η^5-P_5)$_2$] (M = Zn, Cd) are plotted.

As shown in Figure 2, the frontier MOs for the M(η^5-P_5) fragment are singly occupied HOMO [5a, an antibonding combination of the π-(η^5-P_5) orbital in P_5^-(D_{5h}) and the *n*s orbital in the M atom] and a pair of degenerate MOs. However, the frontier MOs for the [M_2(η^5-P_5)$_2$] (M = Zn, Cd) are two degenerate nonbonding doubly occupied HOMO and HOMO-1 and a doubly occupied HOMO-2 ($5a_1$, a M–M bonding MO). The bonding MO of the M–M bond with σ symmetry mostly forms from the weak interaction of the singly occupied HOMOs of two M(η^5-P_5) fragments [partly

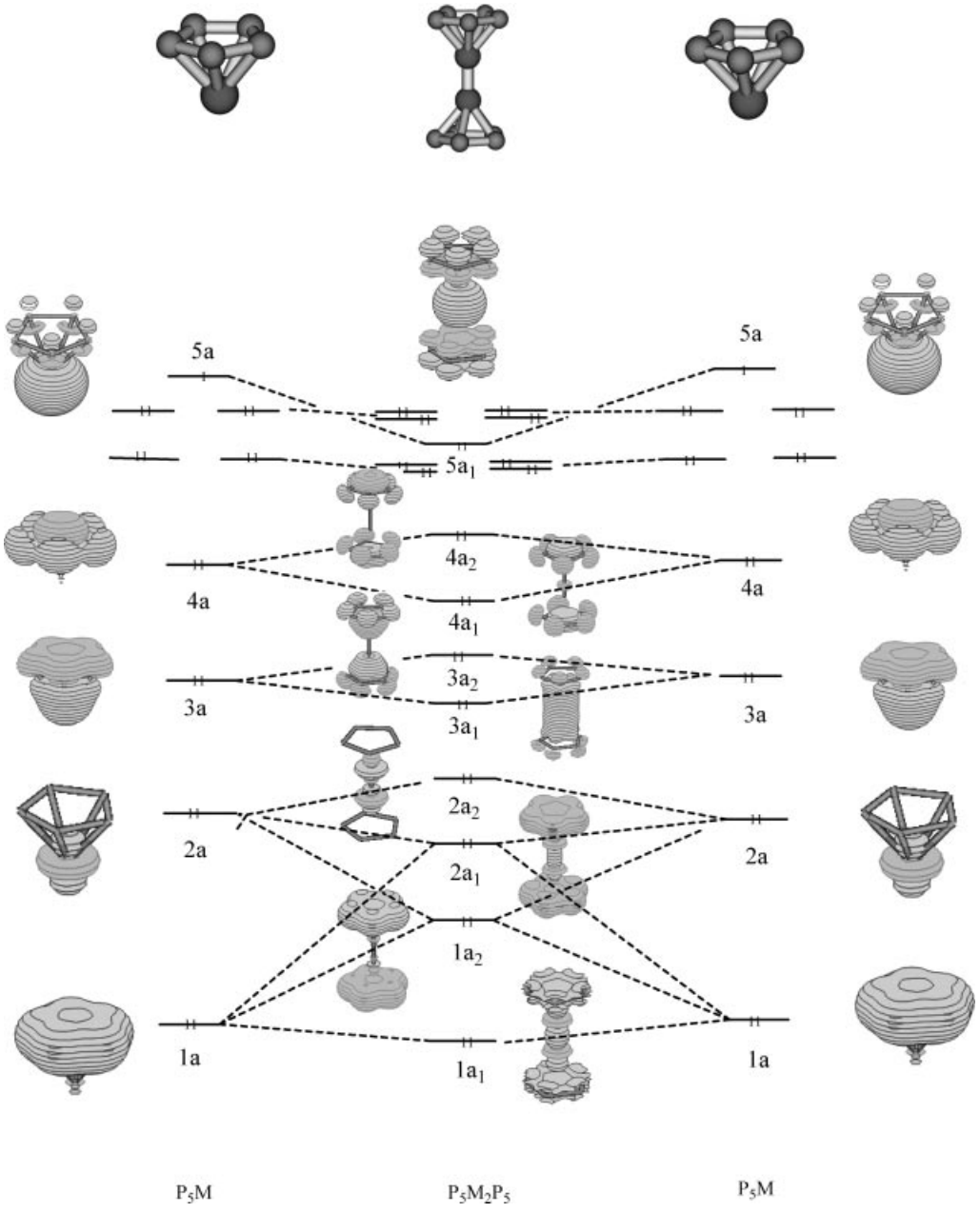

Figure 2. Orbital correlation diagram between the fragments M(η^5-P_5) in (η^5-P_5)M_2(η^5-P_5) and showing the most relevant orbital plots of the fragments M(η^5-P_5) and the correlative molecular orbital plots of (η^5-P_5)M_2(η^5-P_5) (M = Zn, Cd).

 © 2006 Wiley-VCH Verlag GmbH & Co. KGaA, Weinheim

Table 5. Correlative occupied orbital energy differences between the HOMO (5a) in *Ep*M Fragments and the HOMO–2 ($5a_1$) in [$M_2(\eta^5$-$P_5)_2$] {or CpM_2Cp, [$MM'(\eta^5$-$P_5)_2$], Cp $MM'(\eta^5$-$P_5)$ and CpMM′Cp (M, M′ = Zn, Cd)}.

Energy difference	$[Zn_2(P_5)_2]$	$P_5Cd_2P_5$	P_5ZnCdP_5	$CpZn_2P_5$	$CpCd_2P_5$	$CpCdZnP_5$	$CpZn_2Cp$	$CpCd_2Cp$
ΔE_{5a-5a_1} (cal/mol)	55.3	52.4	53.8	59.4	55.0	55.9	59.1	54.9

coming from the interactions of the double occupied 3a, 2a and 1a of the two M(η^5-P_5) fragments and resulting in $3a_1$, $2a_1$, and $1a_1$ MOs as shown in Figure 2, but these weak bonding interactions are counteracted by their antibonding interactions]. Meanwhile, Figure 2 shows that the stabilities of the dinuclear phosphametallocenes correlates with the M–M bond strength, i.e. the magnitude of the MO energy difference (ΔE_{5a-5a_1}) between the singly occupied HOMOs of M(η^5-P_5) fragments and the HOMO–2($5a_1$) representing the M–M bonding orbital in the dinuclear phosphametallocenes correlates with stability of the dinuclear phosphametallocenes. The orbital energy differences (ΔE_{5a-5a_1}) of the phosphametallocenes are listed in Table 5. For comparison, the results of the similar calculations for the CpM_2Cp (D_5 or D_{5h}) (M = Zn, Cd) are listed in Table 3 as well.

As shown in Figure 2 and Table 5, the magnitudes of the orbital energy differences (ΔE_{5a-5a_1}) for the dinuclear phosphametallocenes are very close, and they are slightly smaller than that of the CpM_2Cp (D_5 or D_{5h}). The energy differences among them are small, for example, the ΔE_{5a-5a_1} difference between [$Zn_2(\eta^5$-$P_5)_2$] (D_5) and $CpZn_2Cp$ (D_5) is about 3.8 kcal/mol, and that between [$Cd_2(\eta^5$-$P_5)_2$] (D_5) and $CpCd_2Cp$ (D_{5h}) is only about 2.5 kcal/mol. The magnitude of the orbital energy difference in [$Zn_2(\eta^5$-$P_5)_2$] (D_5) is bigger than that in [$Cd_2(\eta^5$-$P_5)_2$] (D_5), and such energy difference in P_5ZnCdP_5 (C_5)lies between those of [$Zn_2(\eta^5$-$P_5)_2$] (D_5) and [$Cd_2(\eta^5$-$P_5)_2$] (D_5). On the basis of the magnitude of the ΔE_{5a-5a_1}, the order of the stabilities of the dinuclear phosphametallocenes and the dinuclear CpM_2Cp (D_5 or D_{5h}) is that: $CpZn_2P_5$ (C_5) ≈ $CpZn_2Cp$ (D_5) > $CpCdZnP_5$ (C_5) ≈ [$Zn_2(P_5)_2$](D_5) ≈ $CpCd_2P_5$ (C_{5v}) ≈ $CpCd_2Cp$ (D_{5h}) > P_5ZnCdP_5 (C_5) ≈ $P_5Cd_2P_5$ (D_5).

Comparison of the ΔE_{5a-5a_1} ($52.4 \le \Delta E_{5a-5a_1} \le 59.4$ kcal/mol) and the change trends with those of the dissociation energy of the M–M (or M–M′, M, M′ = Zn, Cd) bond ($44.6 \le \Delta E \le 55.4$ kcal/mol) as calculated from equations (1) and (5) (listed in Table 3 and Table 4) reveals that the magnitudes and the change trends of the ΔE_{5a-5a_1} and the dissociation energy of the M–M are very similar. Therefore, the stability of the dinuclear phosphametallocenes correlates with the magnitude of the ΔE_{5a-5a_1}.

The plots of the $3a_1$ and $3a_2$ MO electron density distribution in [$M_2(\eta^5$-$P_5)_2$], derived from the interaction of the unoccupied antibonding e_u of the M_2^{2+} with the doubly occupied 3a, the π bond of $(\eta^5$-$P_5)^-$, shows that there is small amount of orbital overlap between the M_2^{2+} and the $(\eta^5$-$P_5)^-$, thus the covalent interaction between the M_2^{2+} and the (η^5-P_5) plays a secondary role in the stability of [$M_2(\eta^5$-$P_5)_2$], while the electrostatic interaction plays the dominant role. This conclusion is consistent with that the interaction between the M_2^{2+} and the (η^5-P_5) is ionic basing on the analysis of the Laplacian of the electron density.

In addition, the ring currents of the electrons of $4a_1$, $4a_2$, $3a_1$, $3a_2$, $2a_1$, $1a_1$, and $1a_2$ in [$M_2(\eta^5$-$P_5)_2$] as shown in Figure 2 indicate that the dinuclear phosphametallocenes have aromaticity.

4. Aromaticity

The dinuclear phosphametallocenes have equivalent P–P bonds and the charge of the P_5 ring is close to –1 |e| as listed in Tables 1 and 2, which satisfy the geometric criterion of aromaticity and the $(4n+2)\pi$ Hückel's rule.[43] As shown in Figure 2, there are σ ring current[44,45] in the $1a_2$, $1a_1$, $2a_1$, $4a_1$, and $4a_2$ MOs and π ring current in the $3a_1$ and $3a_2$ MOs in $P_5M_2P_5$ (D_5)(M = Zn, Cd). These results indicate that the P_5 rings in the dinuclear phosphametallocenes have aromaticity, and is worthy of further studying on the degree of aromaticity of the complexes.

The NICSs of the optimized structures of the dinuclear phosphametallocenes at the ring center [NICS(0)], at 1 Å above [NICS(1)] and beneath [NICS(–1)] the ring center are computed with GIAO–B3LYP/Gen method. All of the NICSs are listed in Table 6 and Table 7.

NICS has the negative value of the magnetic shielding. It is a simple and efficient aromaticity probe proposed by Schleyer et al.,[46–48] and one of the effective measures of aromaticity recommended by Katritzky et al.[45] This concept has been applied to both organic[46,48] and inorganic compounds,[17,47] transition metal complexes.[49,50] Aromaticity, antiaromaticity, and multiple fold aromaticity,[51] presented in molecules that possess more than one independent

Table 6. Total NICSs (in ppm) for (η^5-P_5)M_2(η^5-P_5), CpM_2(η^5-P_5) and CpM_2Cp (M = Zn, Cd) at GIAO–B3LYP/Gen level of theory.

	$[M_2(P_5)_2]$			$CpM_2(P_5)$				CpM_2Cp		
	P_5^-	$(P_5)Zn$	$(P_5)Cd$	$Zn(P_5)$	CpZn	$(P_5)Cd$	CpCd	Cp	CpZn	CpCd
NICS(0)	–15.4	–15.1	–11.2	–15.4	–14.6	–10.5	–11.1	–12.5	–14.9	–11.5
NICS(1)	–14.8	–15.2	–13.7	–15.0	–11.5	–13.2	–11.0	–9.52	–11.4	–11.9
NICS(–1)	–14.8	–24.4	–11.4	–23.8	–22.4	–10.2	–8.0	–9.52	–23.1	–10.3

 © 2006 Wiley-VCH Verlag GmbH & Co. KGaA, Weinheim

Table 7. Total NICS for (η^5-P_5)ZnCd(η^5-P_5), CpCdZn(η^5-P_5), and CpZnCdCp at GIAO–B3LYP/Gen level of theory.

	$(P_5)ZnCd(P_5)_2$		CpCdZn (P_5)		CpZnCdCp	
	$(P_5)Zn$	$Cd(P_5)$	$(P_5)Zn$	CdCp	CpZn	CpCd
NICS(0)	–15.5	–13.2	–15. 9	–10.9	–15.8	–10.4
NICS(1)	–15.4	–14.3	–15.4	–11.2	–11.5	–11.9
NICS(–1)	–25.6	–14.5	–25.2	–11.1	–24.0	–9.5

delocalized bonding system, either σ-type or π-type, have also been found in the all–metal systems[52,53] and the sandwich–like complexes.[33,38,43,54–57] Recently, we extended NICS to P_5^- and $[Ti(P_5)_2]^{2-}$,[33] and dinuclear metallocene $[CpZn_2Cp]$.[58] Negative NICSs denote aromaticity, positive NICSs denote antiaromaticity, and zero NICS means non-aromaticity. The magnitude of NICSs indicates the degree of aromaticitiy or antiaromaticity.[46,47] According to the dissected NICS analysis on π-aromaticity and antiaromaticity, NICS(1) values (i.e. at 1 Å above) was recommended as better measures of π aromaticity than NICS(0) for benzene (i.e. at the ring centers).[59]

As shown in Table 6 and Table 7, NICS(0), NICS(1) and NICS(–1) in all the dinuclear phosphametallocenes and CpM_2Cp (D_5 or D_{5h}) (M = Zn, Cd) being negative indicates that they are aromatic. However, the differences of NICSs at the same position in different systems reveal that their magnitude of local aromaticity is different. First, the magnitude of NICS(0) in $[M_2(\eta^5\text{-}P_5)_2](D_5)$ is less negative than that in the building block P_5^- (D_{5h}) ion, while NICS(1) and NICS(–1) in $[Zn_2(\eta^5\text{-}P_5)_2](D_5)$ are more negative than those of counterpart in the building block P_5^- (D_{5h}) ion. These are consistent with elongation of the calculated P–P bond lengths. The present calculation predict that the mono-facially coordinated cyclo-P_5 in dinuclear phosphametallocenes undergoes significant ring expansion leading to "loosening of P–P bond " as observed experimentally and calculated theoretically by Malar.[19,32] The consequent loss of local aromaticity in the central cyclo-P_5 indicates that a significant π-electron density can be further transferred from the ring towards the M_2^{2+} unit, such that the positive charge of the M_2^{2+} unit becomes small and the negative charge of cyclo-P_5^- decreases as listed in Table 1 and Table 2. Second, in both the dinuclear phosphametallocenes and CpM_2Cp (D_5 or D_{5h}) (M = Zn, Cd), the magnitude of NICSs in all Zn–(η^5-P_5) (or Zn–Cp) ring plane is more negative than that in all Cd(η^5-P_5) (or Cd–Cp) ring plane, and the magnitude of NICSs in the former (Zn) is more negative than that in the P_5^- (D_{5h})[or $C_5H_5^-$ (D_{5h})] ion. Finally, the magnitude of NICSs in $[M_2(\eta^5\text{-}P_5)_2](D_5)$ is more negative than those in counterpart CpM_2Cp (D_5 or D_{5h}). This may be because that the NICSs in the building block P_5^- (D_{5h}) ion are more negative than those in the building block $C_5H_5^-$ (D_{5h}) ion as listed in Table 6 so that the magnitude of NICSs in $[M_2(\eta^5\text{-}P_5)_2]$ (D_5) is more negative than those in counterpart CpM_2Cp (D_5 or D_{5h}).

We dissected the total NICS values of P_5^- ring in P_5^- (D_{5h}), $[Zn_2(\eta^5\text{-}P_5)_2]$ (D_5) and $[Cd_2(\eta^5\text{-}P_5)_2]$ (D_5) into different P–P bond contributions (σ and π), the M–M bond contribution, the lone pair electrons contributions of P atom and M atom, and the M–(η^5-P_5) bonding contribution are shown in Figures 3, 4 and 5.

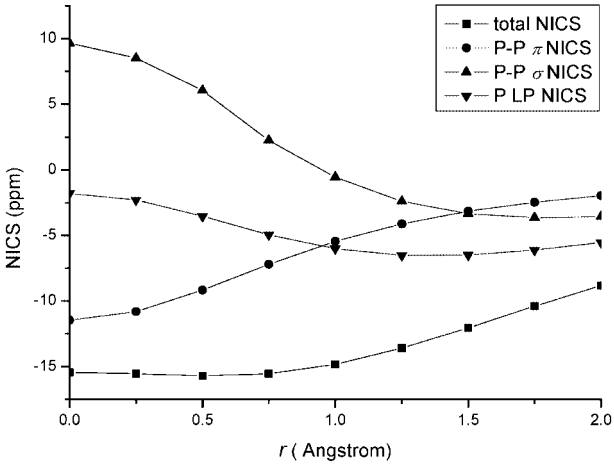

Figure 3. Plot of the NICS contributions of various bonds and total NICS distribution at the center of P_5^-(D_{5h}) ring up to 2.0 Å above at GIAO-B3LYP/+G(2d).

As shown in Figures 3, 4 and 5, although there is a minimum in curves of total NICS distributions of the outer of cyclo- P_5 plane for P_5^- (D_{5h}), $[Zn_2(\eta^5\text{-}P_5)_2]$ (D_5), and $[Cd_2(\eta^5\text{-}P_5)_2]$ (C_5), the magnitude of NICS and the position got the minimum is not complete same, NICS(0.5) = –15.7 ppm for P_5^- (D_{5h}), NICS(0.75) = –15.9 ppm for $[Zn_2(\eta^5\text{-}P_5)_2]$ (D_5), NICS(0.75) = –13.9 ppm for $[Cd_2(\eta^5\text{-}P_5)_2]$ (C_5). This result reveals that the maximal π-electron ring current of the cyclo- P_5 plane in $[M_2(\eta^5\text{-}P_5)_2]$ is shifted from ring center to outer of plane corresponding to P_5^- (D_{5h}). It confirms that there is indeed the expansion of the π-electron density in dinuclear phosphametallocenes again. Therefore, we suggest that the most negative NICS(r) (r may be not equal to 1 Å) should be one of criterion of π aromaticity, too.[33,57]

Comparison of the NICS contributions of various bonds and total NICS distribution in the out-of P_5^- (D_{5h}) plane (as shown in Figure 3) with that in out-of P_5 ring plane of $[Zn_2(\eta^5\text{-}P_5)_2]$ (D_5) [as shown in Figure 4 (a)] indicates that both magnitudes and distributions of total NICS are very similar. Although the NICS contribution of the Zn–Zn bond in $[Zn_2(\eta^5\text{-}P_5)_2]$ (D_5) is positive, and that of Zn–(η^5-P_5) bonding contribution is negative, and the negative contribution slight preponderates the positive contribution, both magnitude and distribution of total NICS in two contributions are very close while the other bond contributions are very close in two contributions. However, the analogous

 © 2006 Wiley-VCH Verlag GmbH & Co. KGaA, Weinheim

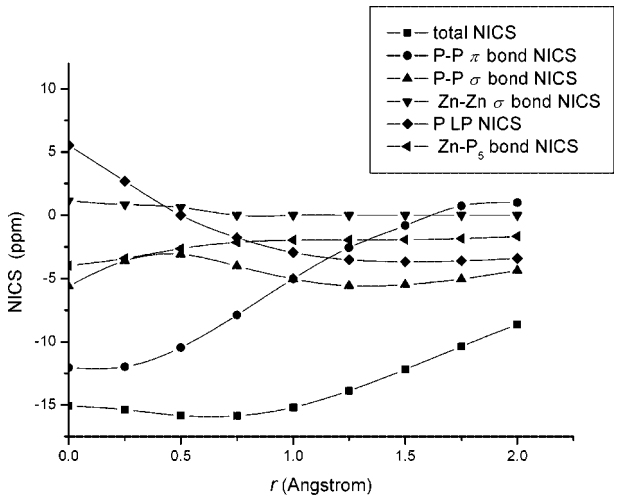

(a)

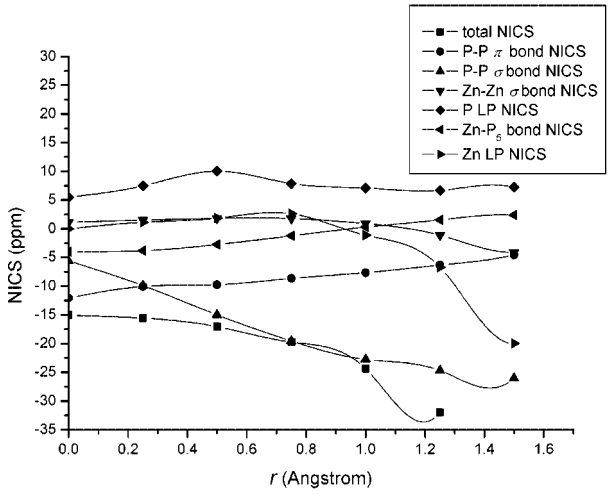

(b)

Figure 4. Plot of the NICS contributions of various bonds and total NICS distribution at the center of P_5^- ring up to 2.0 Å above in $P_5Zn_2P_5$ (D_5) at GIAO-B3LYP/Gen (a) out-of-plane (b) in-plane.

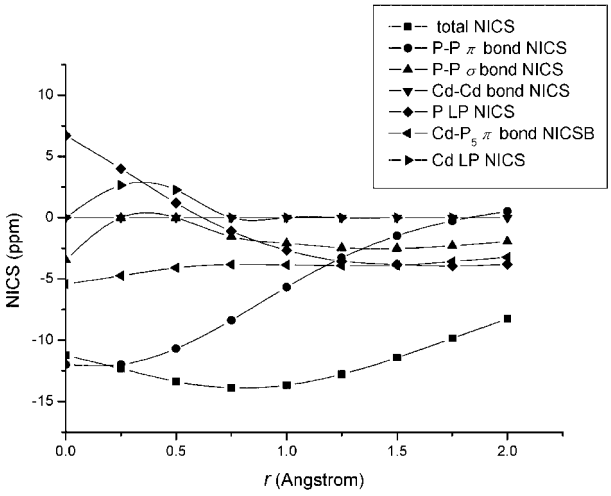

(a)

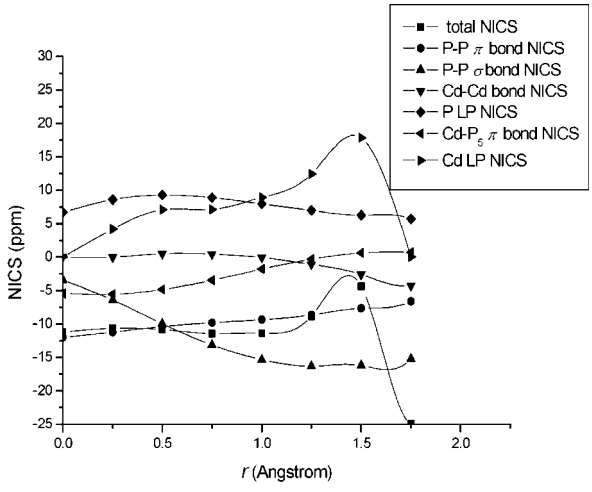

(b)

Figure 5. Plot of the NICS contributions of various bonds and total NICS distribution at the center of P_5^- ring up to 2.0 Å above in $P_5Cd_2P_5$ (D_5) at GIAO-B3LYP/Gen (a) out-of-plane (b) in-plane.

comparison of NICS of out-of P_5^- (D_{5h}) ion plane (as shown in Figure 3) with that of out-of P_5 ring plane of $[Cd_2(\eta^5\text{-}P_5)_2]$ (D_5) [as shown in Figure 5 (a)] reveals that the sum of the positive NICS contribution of the lone pair (LP) electron of Cd atom and of the P–P σ bond preponderates the negative NICS contribution of Cd–(η^5-P_5) bonding while the other bonding NICS contributions are very close. So that the magnitude of total NICS of the out-of P_5 ring plane in $[Cd_2(\eta^5\text{-}P_5)_2]$ (D_5) is not as negative as that of P_5^- (D_{5h}) ion. As for the NICSs of the other dinuclear phosphametallocenes, the magnitude and distribution of total NICS is analogous to that in $[Zn_2(\eta^5\text{-}P_5)_2]$ (D_5) and $[Cd_2(\eta^5\text{-}P_5)_2]$ (D_5). Therefore, the NICSs of the dizinc phosphametallocenes is slightly more negative than that of P_5^- (D_{5h}) ion except for NICS(0), but the NICSs of the dicadmium phosphametallocenes is less negative than that of P_5^- (D_{5h}) ion.

As for the reason that NICS(–1) of the dizinc phosphametallocenes is much more negative than that of the dicadmium phosphametallocenes, as shown in Figure 4 (b) and Figure 5 (b), the curve of total NICS distribution of inner side of the P_5 ring plane in $[M_2(\eta^5\text{-}P_5)_2]$ (D_5) [M = Zn, Cd] drops off with the distance to the M_2^{2+} unit, but the curve of total NICS distribution in $[Zn_2(\eta^5\text{-}P_5)_2]$ (D_5) is much steeper than that in $[Cd_2(\eta^5\text{-}P_5)_2]$ (D_5), so that the distribution curves of NICS contributions of in-P_5-ring

 © 2006 Wiley-VCH Verlag GmbH & Co. KGaA, Weinheim

plane for the Zn–Zn bond, the LP of Zn, and the P–P σ bond in $[Zn_2(\eta^5\text{-}P_5)_2]$ (D_5) is much steeper than that of the Cd–Cd bond, the LP of Cd, and the P–P σ bond in $[Cd_2(\eta^5\text{-}P_5)_2]$ (D_5). Therefore, the magnitude of total NICS of inner side of the P_5 ring plane in $[Zn_2(\eta^5\text{-}P_5)_2]$ (D_5) is much more negative than that in $[Cd_2(\eta^5\text{-}P_5)_2]$ (D_5) at the same position, the NICS(–1) of $[Zn_2(\eta^5\text{-}P_5)_2]$ (D_5) is much more negative than that of $[Cd_2(\eta^5\text{-}P_5)_2]$ (D_5). The NICS(–1) of other dinuclear phosphametallocenes has similar phenomena.

5. Conclusions

The analysis of energy and the harmonic frequencies on the equilibrium geometries of both series of dinuclear phosphametallocenes, $[MM'(\eta^5\text{-}P_5)_2]$ and $(\eta^5\text{-}P_5)MM'Cp$ (M, M′ = Zn, Cd), shows that all the minima of the dinuclear phosphametallocenes with singlet electronic state have an staggered ($9° \leq D_{(E\text{–}M\text{–}M\text{–}E')} \leq 36°$) conformation except for the eclipsed $CpCd_2(P_5)$ (C_{5v}, $D_{(E\text{–}M\text{–}M\text{–}E')} = 0°$), and all the D_{5h} and the D_{5d} symmetric conformations are transition states while the energy differences between the most stable minimum and the transition states are very small (≤ 0.1 kcal/mol). The rotation of P_5 ring about the M–M bond in all complexes is almost free.

The analyses of the NBO, the Laplacian of the electron density, the electrostatic interaction energy, the bonding energy decomposition, and the MO correlation diagrams for the two series complexes reveal that the properties of all the dinuclear phosphametallocenes are similar to that of the dizinc metallocenes. The M–M (or M–M′) bond in the dinuclear phosphametallocenes is a weak σ covalent bond, and the magnitude of bonding energy of the M–M (or M–M′) bond correlates with the energy difference between the energy of HOMO in $M(\eta^5\text{-}P_5)$ [or MCp] (^2A, C_{5v}) fragment and the energy of HOMO–2 in $[MM'(\eta^5\text{-}P_5)_2]$ (^1A, D_5, or D_{5h}) [or $(\eta^5\text{-}P_5)MM'Cp$ (^1A, C_5 or C_{5v})] (M, M′ = Zn, Cd). The M–M (or M–M′) bond strength plays a dominant role in the stability of the dinuclear phosphametallocenes. On the other hand, the M–(η^5-P_5) [or M–Cp] bonding is mainly ionic. Among the different dinuclear phosphametallocenes with the same ligands, the bonding energies of the M–M (or M–M′) bond and the M–(η^5-P_5) (or M–Cp) bonds decrease as M varying from Zn to Cd. However, among the different dinuclear phosphametallocenes with the same metal, the bonding energies of the M–M (or M–M′) bond and the M–ligand bonds increase as ligand varying from (η^5-P_5) to Cp.

The negative NICSs indicate that all dinuclear phosphametallocenes have aromaticity. The various dissected bond NICS contributions reveal that the NICS contributions of the metal–ligand bond, the metal–metal bond and the metal lone pair electrons to the overall aromaticity in the Zn-containing dinuclear phosphametallocenes are different from their counterpart contributions in the Cd-containing dinuclear phosphametallocenes, such difference causes that the overall NICSs of the Zn-containing dinuclear phosphametallocenes are more negative than that of the Cd-containing dinuclear phosphametallocenes.

Acknowledgments

This research was supported by the National Nature Science Foundation of China (no. 20473031) and the Key Laboratory for Supramolecular Structure and Material of Jilin University. W. Q. T. thanks Japan Society for the Promotion of Science for financial support and is grateful to Professor Yuriko Aoki for her hospitality.

[1] I. Resa, E. Carmona, E. Gutierrez-Puebla, A. Monge, *Science* **2004**, *305*, 1136–1138.
[2] D. d. Río, A. Galindo, I. Resa, E. Carmona, *Angew. Chem. Int. Ed.* **2005**, *44*, 1244–1247.
[3] G. Parkin, *Science* **2004**, *305*, 1117–1118.
[4] A. Schnepf, H.-J. Himmel, *Angew. Chem. Int. Ed.* **2005**, *44*, 3006–3008.
[5] A. Schnepf, H.-J. Himmel, *Angew. Chem.* **2005**, *117*, 3066–3068.
[6] S. L. Richardson, T. Baruah, M. R. Pederson, *Chem. Phys. Lett.* **2005**, *404*, 141 –145.
[7] Y.-M. Xie, H. F. Schaefer III, R. B. King, *J. Am. Chem. Soc.* **2005**, *127*, 2818–2819.
[8] Z.-Z. Xie, W. H. Fang, *Chem. Phys. Lett.* **2005**, *404*, 212–216.
[9] H. Wang, Y.-M. Xie, R. B. King, H. F. Schaefer III, *J. Am. Chem. Soc.* **2005**, *127*, 11646–11651.
[10] Y.-M. Xie, H. F. Schaefer III, E. D. Jemmis, *Chem. Phys. Lett.* **2005**, *402*, 414–421.
[11] A. Y. Timoshkin, H. F. Schaefer, *Organometallics* **2005**, *24*, 3343–3345.
[12] H. S. Kang, *J. Phys. Chem. A* **2005**, *109*, 4342–4351.
[13] O. J. Scherer, T. Brück, *Angew. Chem. Int. Ed. Engl.* **1987**, *26*, 59–59.
[14] M. Baudler, S. Akpapoglou, H. Budzikiewicz, H. Münster, *Angew. Chem. Int. Ed. Engl.* **1988**, *27*, 280–281.
[15] P. H. Tracy, H. F. Schaefer III, *Angew. Chem. Int. Ed. Engl.* **1989**, *28*, 485–486.
[16] E. J. P. Malar, *J. Org. Chem.* **1992**, *57*, 3694–3698.
[17] A. Dransfeld, L. Nyulászi, P. v. R. Schleyer, *Inorg. Chem.* **1998**, *37*, 5600–5606.
[18] H.-J. Zhai, L.-S. Wang, A. E. Kuznetsov, A. I. Boldyrev, *J. Phys. Chem. A* **2002**, *106*, 5600–5606.
[19] E. J. P. Malar, *Eur. J. Inorg. Chem.* **2004**, 2723–2732.
[20] F. D. Proft, P. W. Fowler, R. W. A. Havenith, P. v. R. Schleyer, G. V. Lier, P. Geerlings, *Chem. Eur. J.* **2004**, *10*, 940–950.
[21] Q. Jin, B. Jin, G. W. Xu, W. Zhu, *J. Mol. Struct. (THEOCHEM.)* **2005**, *713*, 113–117.
[22] E. J. P. Malar, *Inorg. Chem.* **2003**, *42*, 3873–3883.
[23] Ê. D. V. Bruce, R. R. Willian, *Organometallics* **2004**, *23*, 5308–5313.
[24] J. A. Chamizo, M. R. Mazőn, R. Salcedo, R. A. Tosano, *Inorg. Chem.* **1990**, *29*, 879–880.
[25] R. F. Winter, W. E. Geiger, *Organometallics* **1999**, *18*, 1827–1833.
[26] F. G. N. Cloke, J. C. Green, J. R. Hanks, J. F. Nixon, J. L. Suter, *J. Chem. Soc., Dalton Trans.* **2000**, 3534–3536.
[27] M. Lein, J. Frunzke, A. Timoshkin, G. Frenking, *Chem. Eur. J.* **2001**, *7*, 4155–4163.
[28] J. Frunzke, M. Lein, G. Frenking, *Organometallics* **2002**, *21*, 3351–3359.
[29] V. M. Rayón, G. Frenking, *Chem. Eur. J.* **2002**, *8*, 4693–4707.
[30] A. R. Kudinov, D. A. Loginov, Z. A. Starikova, P. V. Petrovskii, M. Corsini, P. Zanello, *Eur. J. Inorg. Chem.* **2002**, 3018–3027.
[31] M. Lein, J. Frunzke, G. Frenking, *Angew. Chem. Int. Ed.* **2003**, *42*, 1303–1306.
[32] E. J. P. Malar, *Theor. Chem. Acc.* **2005**, *114*, 213–221.
[33] Z.-Z. Liu, W. Q. Tian, J.-K. Feng, G. Zhang, W.-Q. Li, *J. Phys. Chem. A* **2005**, *109*, 5645–5655.
[34] E. Urnėžius, W. W. Brennessel, C. J. Cremer, J. E. Ellis, P. v. R. Schleyer, *Science* **2002**, *295*, 832–834.

 © 2006 Wiley-VCH Verlag GmbH & Co. KGaA, Weinheim

[35] M. Lein, J. Frunzke, G. Frenking, *Inorg. Chem.* **2003**, *42*, 2504–2511.
[36] U. Koch, P. L. A. Popelier, *J. Phys. Chem.* **1995**, *99*, 9747–9757.
[37] P. L. A. Popelier, *J. Phys. Chem. A* **1998**, *102*, 1873–1878.
[38] W. Chen, Z.-R. Li, D. Wu, Y. Li, C.-C. Sun, *J. Chem. Phys.* **2005**, *123*, 164306–164311.
[39] Gaussian NBO version 3.1: E. D. Glendening, A. E. Reed, J. E. Carpenter, F. Weinhold, Theoretical Chemistry Institute and Department of Chemistry, University of Wisconsin, **1990**.
[40] M. J. Frisch, G. W. Trucks, H. B. Schlegel, G. E. Scuseria, M. A. Robb, J. R. Cheeseman, J. A.Montgomery Jr, T. Vreven, K. N. Kudin, J. C. Burant, J. M. Millam, S. S. Iyengar, J. Tomasi, V. Barone, G. Cossi; Scalmani, N. Rega, G. A. Petersson, H. Nakatsuji, M. Hada, M. Ehara, K. Toyota, R. Fukuda, J. Hasegawa, M. Ishida, T. Nakajima, Y. Honda, O. Kitao, H. Nakai, M. Klene, X. Li, J. E. Knox, H. P. Hratchian, J. B. Cross, C. Adamo, J. Jaramillo, R. Gomperts, R. E. Stratmann, O. Yazyev, A. J. Austin, R. Cammi, C. Pomelli, J. W. Ochterski, P. Y. Ayala, K. Morokuma, G. A. Voth, P. Salvador, J. J. annenberg, V. G. Zakrzewski, S. Dapprich, A. D. Daniels, M. C. Strain, O. Farkas, D. K. Malick, A. D. Rabuck, K. Raghavachari, J. B. Foresman, J. V. Ortiz, Q. Cui, A. G. Baboul, S. Clifford, J. Cioslowski, B. B. Stefanov, G. Liu, A. Liashenko, P. Piskorz, I. Komaromi, R. L. Martin, D. J. Fox, T. Keith, M. A. Al-Laham, C. Y. Peng, A. Nanayakkara, M. Challacombe, P. M. W. Gill, B. Johnson, W. Chen, M. W. Wong, C. Gonzalez, J. A. Pople, *Gaussian 03*, Revision B.03, Gaussian, Inc., Pittsburgh PA, **2003**.
[41] G. Schaftenaar, J. H. J. Noordik, *J. Comput. Aided Mol. Des.* **2000**,*14*, 123.
[42] At present, some scientists differentiate the type of chemical bonds using the Laplacian of the electron density of the bond critical points (BCPs). For ionic bonds, hydrogen bonds, and van der Waals interactions, the Laplacian of the electron density $\nabla^2\rho(r)$ is positive, while the $\nabla^2\rho(r_{Ep-M})$ is negative for covalent bond. We think that the $\nabla^2\rho(r_{Ep-M})$ near to zero indicates both ionic bond and covalent bond.
[43] E. D. Jemmis, P. v. R. Schleyer, *J. Am. Chem. Soc.* **1982**, *104*, 4781.
[44] K. Jug, *J. Org. Chem.* **1983**, *48*, 1344–1348.
[45] A. R. Katritzky, K. Jug, D. C. Oniciu, *Chem. Rev.* **2001**, *101*, 1421–1449.
[46] P. v. R. Schleyer, C. Maerker, A. Dransfeld, H. Jiao, N. J. R. V. E. Hommes, *J. Am. Chem. Soc.* **1996**, *118*, 6317–6318.
[47] P. v. R. Schleyer, H.-J. Jiao, N. J. R. v. E. Hommes, V. G. Malkin, O. L. Malkina, *J. Am. Chem. Soc.* **1997**, *119*, 12669–12670.
[48] T. Heine, P. v. R. Schleyer, C. Corminboeuf, G. Seifert, R. Reviakine, J. Weber, *J. Phys. Chem. A* **2003**, *107*, 6470–6475.
[49] A. C. Tsipis, C. A. Tsipis, *J. Am. Chem. Soc.* **2003**, *125*, 1136–1137.
[50] P. v. R. Schleyer, B. Kiran, D. V. Simion, T. S. Sorensen, *J. Am. Chem. Soc.* **2000**, *122*, 510–513.
[51] E. D. Jemmis, P. v. R. Schleyer, *J. Am. Chem. Soc.* **1982**, *104*, 4781–4788.
[52] J. M. Mercero, J. M. Ugalde, *J. Am. Chem. Soc.* **2004**, *126*, 3380–3381.
[53] Z.-F. Chen, C. Corminboerf, T. Heine, J. Bohmann, P. v. R. Schleyer, *J. Am. Chem. Soc.* **2003**, *125*, 13930–13931.
[54] J. M. Mercero, J. M. Matxain, J. M. Ugalde, *Angew. Chem. Int. Ed.* **2004**, *43*, 5485–5488.
[55] S.-D. Li, J.-C. Guo, C.-Q. Miao, G.-M. Ren, *Angew. Chem.* **2005**, *117*, 2–5.
[56] S.-D. Li, J.-C. Guo, C.-Q. Miao, G.-M. Ren, *Angew. Chem. Int. Ed.* **2005**, *44*, 2158–2161.
[57] Ê. D. V. Bruce, W. Rocha, *Organometallics* **2004**, *23*, 5308–5313.
[58] Z.-Z. Liu, W. Q. Tian, J.-K. Feng, G. Zhang, W.-Q. Li, *J. Mol. Struct. (THEOCHEM)* **2006**, *758*, 127–138.
[59] P. v. R. Schleyer, M. Manoharan, Z.-X. Wang, B. Kiran, H. Jiao, R. Puchta, N. J. R. van Eikema Hommes, *Org. Lett.* **2001**, *3*, 2465–2468.

Received: December 26, 2005
Published Online: May 3, 2006

 © 2006 Wiley-VCH Verlag GmbH & Co. KGaA, Weinheim